

**Thermionic emission and work function of multiwalled carbon nanotube yarns**

Peng Liu, Yang Wei, Kaili Jiang,\* Qin Sun, Xiaobo Zhang, and Shoushan Fan†

*Department of Physics and Tsinghua-Foxconn Nanotechnology Research Center, Tsinghua University, Beijing 100084, China*

Shufeng Zhang, Chuangang Ning, and Jingkang Deng

*Department of Physics, Tsinghua University, Beijing 100084, China*

(Received 10 February 2006; revised manuscript received 21 April 2006; published 15 June 2006)

Thermionic emission from multiwalled carbon nanotubes (MWNTs) was investigated by using MWNT yarns. The work function of MWNT and thermionic emission constant of the yarn sample were both calculated from the thermionic emission data. The measured work function of MWNT is about 4.54–4.64 eV. The emission constant is larger than conventional thermionic cathode. Thermionic emission electron energy spectra at various temperatures have also been measured by using the MWNT yarn as the thermionic cathode in an electron momentum spectra instrument. The full width at half maximum of the spectra show a linear relation with the temperature. The carbon nanotube yarn may be used as thermionic cathode to replace the conventional cathode for their special properties.

DOI: [10.1103/PhysRevB.73.235412](https://doi.org/10.1103/PhysRevB.73.235412)

PACS number(s): 81.07.De, 73.30.+y, 79.40.+z, 79.70.+q

**I. INTRODUCTION**

Thermionic and field electron emission phenomena have been studied for a long time and are widely applied in scientific instruments nowadays. Due to their distinguished electrical conducting capability, high aspect ratio, chemical inertness, and structural stability, carbon nanotubes (CNTs) possess a great potential in field emission applications such as field emitters in flat panel displays and other vacuum electronic devices. Consequently, field electron emission from CNTs has been intensely studied.<sup>1–3</sup> Since the work function of CNTs is the most fundamental parameter in field emission, many efforts have been put on measuring or calculating it.<sup>4–17</sup> As is well known, there are three commonly adopted methods to measure the work function, namely contact potential difference (CPD), photoelectron emission spectroscopy (PEES), and thermionic emission (TE).<sup>18</sup> CPD (Refs. 12 and 13) and PEES (Refs. 7–11) have been employed to measure the work function of CNTs. However, there is no CNTs work function data derived from TE method until now. The difficulty lies in how to eliminate the thermionic emission from the heating element if it is not made of pure CNTs.

In 2002, we had developed a method to prepare super-aligned multiwalled nanotube (MWNT) arrays from which continuous pure MWNT yarns can be directly drawn like silk being drawn from a silkworm cocoon.<sup>19</sup> After this, Baughman's group developed a draw-twisting method to make it a rope,<sup>20</sup> then they demonstrated more applications such as transparent conducting film.<sup>21</sup> Recently, the synthesis has been expanded to 4 in. wafer scale and a new method was invented to process raw yarns. The processed yarn is both elastic and pliable, and can be easily manipulated and shaped to any desired shape,<sup>22</sup> which gives us great convenience for experimental study. Also the pure yarn can be current heated to incandescence in vacuum and the temperature can be precisely determined by fitting the luminescence spectra with black body radiation.<sup>23</sup> We therefore are able to study the TE from MWNTs. Here we show our investigation of the TE from MWNTs, from which the work function of MWNTs was determined, ranging from 4.54–4.64 eV. The thermionic

emission constant of the yarn sample has also been calculated. We found it is larger than that of the conventional metal thermionic cathode. We also measured the thermionic emission electron energy spectra at various temperatures by using the MWNT yarn as the thermionic cathode in an electron momentum spectra instrument. The full width at half maximum (FWHM) of the spectra shows a linear relation with temperature.

**II. THERMIONIC EMISSION AND DETERMINATION OF THE WORK FUNCTION**

The freshly drawn MWNT yarns appear as very thin ribbon of several microns thick and several centimeters wide.<sup>19,22</sup> After passing through ethanol, the MWNT yarn shrinks to a thin thread typically 20–30 microns in diameter, in which MWNTs form a tight bundle.<sup>22</sup> This treated yarn shows good mechanical properties and can be easily manipulated by hand.<sup>22</sup> A 2 cm long treated yarn was cut from our continuous yarn, and then bent to an angle shape. After that, two arms of the angle-shaped emitter were mounted on two nickel rods, respectively. To ensure good contacts between yarn and electrode, we first rolled the yarn on the nickel rod to increase the contact area and then silver paste was used to fix it and further improve the contact. The measured resistance of 2 cm long yarn is only 500  $\Omega$ , and there is no obvious overheating near the contact points. A molybdenum plate facing the angle-shaped yarn is used as the anode. The anode voltage is applied by a source meter (Keithley 237), which can simultaneously measure the emission current. Figure 1(a) is the schematic diagram of the electric circuit. The MWNT yarn can be uniformly heated up by passing a current through it. Figure 1(b) shows the optical image of the heated yarn. A spectrum analyzer (Konica-Minolta CS-1000A) was utilized to acquire the luminescence spectra of the heated yarn. The temperature can be accurately measured by fitting the spectra with that of black body radiation as we have reported.<sup>23</sup> Figure 2(a) is a scanning electron microscopy (SEM) image of a typical tip of the angle-shaped yarn,

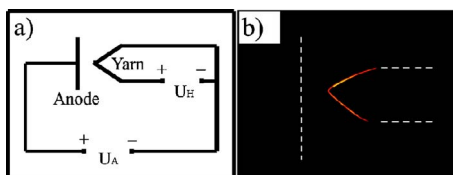


FIG. 1. (Color online) (a) Schematic electric circuit of the experimental setup. (b) Optical image of the MWNT yarn, heated to a temperature of 1333 K by a dc current. The image is taken by a digital camera at F2.0, 1/80 s shutter. The dashed white lines indicate the positions of the electrodes.

which is the cathode emitter. Figure 2(b) is the typical high resolution transmission electron microscope (HRTEM) image of the MWNT used in our experiment. The experiment is carried out in a vacuum chamber of base pressure  $5 \times 10^{-6}$  Pa.

Figure 3(a) displays the measured electron emission  $I$ - $V$  curve of the MWNT yarn at various temperatures. According to our room temperature field emission data, there is no visible field emission current at a voltage below 200 V. We therefore attribute the high temperature emission currents below 200 V to thermionic emission. The thermionic emission can be further divided into two regimes. At voltages below about 30 V [Fig. 3(a)], the emission current changes drastically with voltages, which is called retarding field regime. Above 30 V, the emission current follows a saturationlike behavior, which is called accelerating field regime. It is clear that the higher the temperature, the larger the saturated current in this regime. However, the thermionic emission current is not truly saturated, but increases slowly with anode voltage increasing due to the Schottky effect,<sup>24</sup> i.e., the lowering of work function caused by applied electric field. When the voltage and temperature are both high enough, the emis-

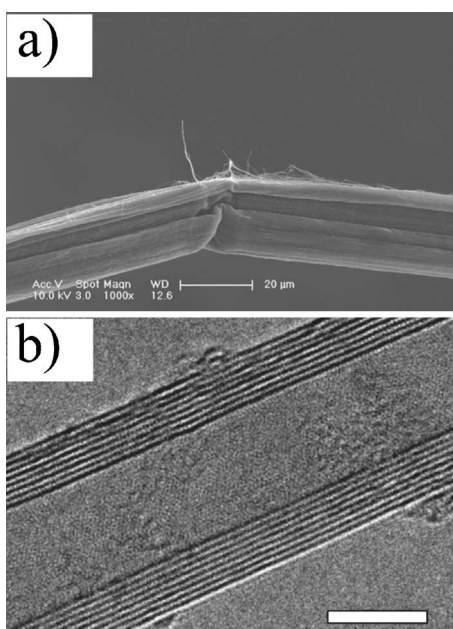


FIG. 2. (a) The typical SEM image of a MWNT yarn emitter, taken at 1000 $\times$ ; scale bar is 20  $\mu$ m. (b) The HRTEM image of a MWNT derived from the yarn; scale bar is 5 nm.

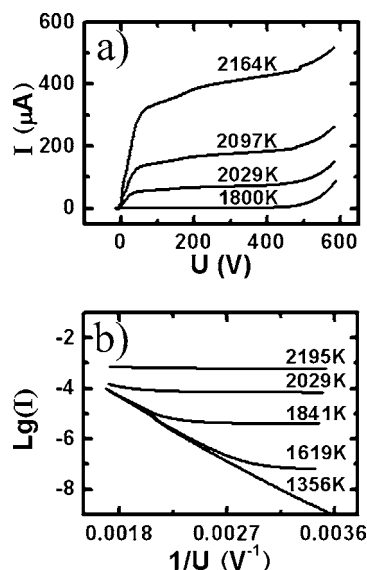


FIG. 3. (a) The  $I$ - $V$  curve at the full voltage region. (b) Typical thermal field emission curves, similar to the earlier calculation by Dyke and Dolan (Ref. 25).

sion enters into the so-called thermal field emission. Note that the field emission starts at a low voltage as little as 400 V, which implies a large field enhancement factor. Therefore the thermionic emission is mainly coming from the yarn’s surface, but the field emission is coming from a few MWNTs’ tips protruding out of the yarn [see Fig. 2(a)]. Figure 3(b) is a plot of  $\lg I$  versus inverse of voltage, which is usually utilized to characterize the thermal field emission. The curves have the same feature as the thermal field emission from tungsten formerly investigated by Dolan and Dyke.<sup>25</sup> (In this paper, “lg” represents logarithms to the base 10.)

For thermionic emission, the emission current density depends on the work function and temperature of the cathode, which can be described by the famous Richardson’s formula<sup>26</sup>

$$j_0 = AT^2 \exp\left[-\frac{\phi}{kT}\right]. \tag{1}$$

Here  $j_0$  is the zero-field current density,  $A$  is the Richardson’s emission constant,  $T$  is the absolute temperature,  $\phi$  is the work function of cathode at absolute zero temperature, and  $k$  is Boltzmann constant. If we have the zero-field current density value at various temperatures, we will be able to obtain the work function of the MWNT from the slope of  $\lg j_0/T^2$  versus  $1/T$ .

Here we use the Schottky effect to determine the zero field emission current density  $j_0$ . The emission current density versus external electric field in the accelerating field region can be expressed as<sup>24</sup>

$$j_a = j_0 \exp\left[\frac{e \sqrt{\frac{e\mathcal{E}}{4\pi\epsilon_0}}}{kT}\right]. \tag{2}$$

Here  $j_a$  is the anode current density,  $e$  the electron charge,  $\mathcal{E}$  is the external electric field, and  $\epsilon_0$  the vacuum dielectric

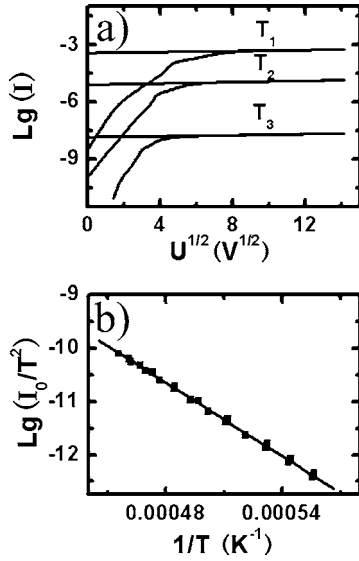


FIG. 4. (a) The  $\lg I - \sqrt{U}$  curve. The straight lines represent the results of linearly fitting in accelerating region. (b) Experimental data (solid square) and fitted line in  $\lg I_0/T^2$  versus  $1/T$  plot.

constant. Conducting logarithm operation on both sides, we obtain the following expression:

$$\lg j_a = \lg j_0 + 1.906 \frac{\sqrt{\mathcal{E}}}{T}. \quad (3)$$

$\mathcal{E}$  can be assumed as  $\alpha(U_a + U_c)$ ,  $U_a$  is anode voltage in V,  $U_c$  is contact potential between the cathode and anode, and  $\alpha$  is a constant in  $\text{cm}^{-1}$  determined by the electrode geometry, then Eq. (3) can be expressed as

$$\lg j_a = \lg j_0 + 1.906 \frac{\sqrt{\alpha}}{T} \sqrt{(U_a + U_c)}. \quad (4)$$

It is clear that if we plot  $\lg j_a$  against  $\sqrt{U_a + U_c}$ , by linearly fitting the curve, the intercept on the y axis should be  $\lg j_0$ . Because the work function of the anode material, molybdenum, is 4.21 eV, which is very close to that of graphite, 4.6 eV. Therefore we can neglect the contact potential between anode and cathode  $U_c$ , just linearly fitting  $\lg j_a$  against  $\sqrt{U_a}$  to get  $\lg j_0$ . In practice, we do linear fit on  $\lg I_a$  versus  $\sqrt{U_a}$  and get the zero field current  $\lg I_0$ , as is shown in Fig. 4(a). By linearly fitting  $\lg I_0/T^2$  versus  $1/T$ , we can obtain the work function of the MWNT yarn as shown in Fig. 4(b). Here,  $\lg I_0 = \lg(j_0 S)$ ,  $S$  is the emission area, which can be estimated by assuming the cathode as a 20  $\mu\text{m}$  diameter and 2 cm length wire.  $S$  is included in the intercept of curve  $\lg I_0/T^2$  versus  $1/T$ , and will influence the Richardson's

emission constant. However,  $S$  does not influence the slope of  $\lg I_0/T^2$  versus  $1/T$  and the work function.

### III. RESULT AND DISCUSSION

Four different samples have been investigated in a temperature range of 1500–2200 K, of which the derived work functions are between 4.54–4.64 eV (see Table I). The thermionic emission constants are also included in the table. In the experimental literature,<sup>4–15</sup> the reported work functions of MWNTs scattered from less than 1.0 to 7.3 eV, which are mainly derived from four methods.

The first method is based on fitting the field emission data with the Fowler-Nordheim (FN) equation.<sup>4–6</sup> However this method has been pointed out to be unsuitable for determining MWNT's work function,<sup>9</sup> because the estimation of enhancement factor usually introduces large uncertainty.

The second method is based on the measurement of contact potential difference (CPD) between CNT and a reference electrode,<sup>12,13</sup> which is a relative measurement. Cui and colleagues determined the work function of SWNT to be 0.1 eV higher than highly oriented pyrolytic graphite (HOPG).<sup>12</sup> By using gold as reference electrode, Gao and colleagues obtained MWNTs' work function with a large variation (4.6–5.6 eV).<sup>13</sup>

The third method is involved in using photoelectron emission spectroscopy (PEES) to determine the MWNT's work function. Many groups have employed PEES to determine the work function of both HOPG and CNTs.<sup>7,9,8,10</sup> However, their results also show a relatively large variation in both HOPG (4.4–4.8 eV) and CNTs (4.3–5.05 eV).

The fourth method is based on measuring the energy spectra of field emission electrons, as is shown by Gröning *et al.* in Refs. 11 and 14. Their result is  $5 \pm 0.3$  eV for MWNT. However, this method adopted the free electron model to approximate the true density of states particularly for carbon, which can also affect the result.<sup>27</sup>

Here we would like to stress two points in measuring the work function of CNTs. The first is that the adsorbates on CNT tip will alter the work function. According to Refs. 28 and 29 and our results, the adsorption of water molecule will result in a decrease in work function. We also found that adsorption of organic molecules on the CNT tip will result in a higher work function. Therefore to accurately measure the work function, a desorption step in vacuum is imperative. The second point is that different graphitization level of CNTs also give rise to different work functions. According to Ago and colleagues,<sup>7</sup> plasma oxidized CNTs resulted in amorphous carbon deposition on CNTs, which will further increase the work function substantially. Therefore, to mea-

TABLE I. The measured work function and corresponding temperature range.

Sample number	1	2	3	4
Work function (eV)	4.64	4.61	4.63	4.54
Richardson's emission constant ( $\text{A cm}^{-2} \text{K}^{-2}$ )	824	579	807	228
Temperature range (K)	1523—2118	1489—2207	1497—2188	1468—2195

sure the intrinsic work function of CNTs, thermal annealing, or air oxidization is suggested to remove amorphous carbon. In this study, both requirements are automatically fulfilled by thermionic emission, which is the merit of the TE method.

However, our approach shown here also has deficiency. According to Zhou and colleagues,<sup>30</sup> the local density of states at the tip make the work function different from the sidewalls. Since the yarn is composed of end-to-end jointed MWNTs, the measured thermionic emission current was contributed by both sidewalls and tips. In principle, the work function we measured should be a mixture of sidewalls and tips. Fortunately, due to the small area of tip (10 nm diameter) and long length of MWNTs (several hundreds of microns), a majority of the thermionic emission currents was contributed by the sidewalls. Therefore the work functions we measured here are mainly attributed to the sidewalls of MWNT.

As to Richardson's emission constant, theoretical value is  $120.4 \text{ A cm}^{-2} \text{ K}^{-2}$ .<sup>24</sup> Experimentally determined constants for real metals are smaller than this value.<sup>18</sup> However we can see that the measured values in our experiment are all larger than the theoretical result. This may be due to the rough estimation of emission area. The theoretical calculation for emission constant is based on a smooth surface metal, while the surface roughness of the cathode will increase the emission area and the emission constant,<sup>31</sup> which is just the case for CNT yarns.

#### IV. ENERGY SPECTRA OF THERMIONIC ELECTRONS FROM CNT

The yarn is used as the thermal emission cathode of an electron momentum spectroscopy instrument. Figure 5(a) shows the structure of cathode part. CNTs yarns replaced the tungsten cathode. The energy spectra of thermal emitted electrons were measured at various temperatures. Fig. 5(b) is a typical energy spectrum at 2024 K and shows a FWHM about 0.8 eV. The inset of Fig. 5(b) is the relation between the FWHM and temperature. The FWHM increases linearly with temperature, which is in good accordance with theoretical predictions.<sup>18,24</sup> Because CNTs have almost the same work function as tungsten, their FWHMs are very close. Compared with tungsten, CNT yarn has the merits of structural stability, chemical inertness, and high emission constant, which makes it a good candidate to replace the tungsten wire cathode in commercial instruments.

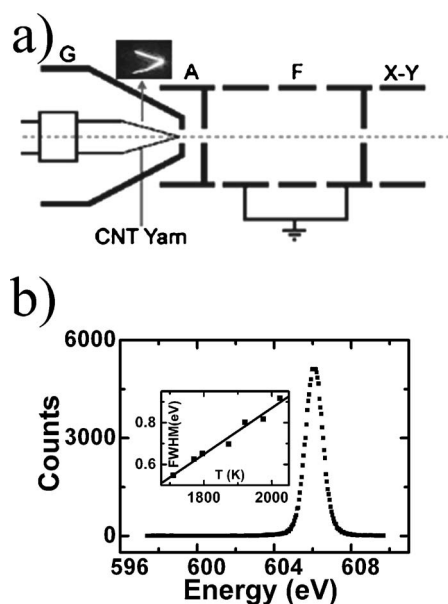


FIG. 5. (a) The carbon nanotubes yarn was used in the electron momentum spectrum instrument as the cathode. (b) The typical energy spectra of thermionic emission. In the inset is the curve of FWHM with temperature.

#### V. CONCLUSION

In conclusion, by using MWNT yarn we have measured the work function of CVD-grown MWNT, which ranges from 4.54 to 4.64 eV. The yarn shows a larger emission constant than the conventional thermionic cathodes. The energy spectra of thermionic emission at various temperatures have also been measured by using the MWNT yarn as the thermionic cathode in an electron momentum spectra instrument. The FWHM of the spectra show a linear relation with the temperature. The MWNT yarn may be used as thermionic cathode to replace the conventional tungsten cathode.

#### ACKNOWLEDGMENTS

We acknowledge discussion with Pijin Chen, Zhaofu Hu, and Huan Cheng. We also thank Jing Kong and Wenhui Duan for both valuable suggestions and proofreading. We acknowledge the financial support from the National Basic Research Program of China (Grant No. 2005CB623606) and NSFC (Grant Nos. 10334060 and 10575062).

\*Electronic address: jiangkl@tsinghua.edu.cn

†Electronic address: fss-dmp@tsinghua.edu.cn

<sup>1</sup>R. H. Baughman, A. A. Zakhidov, and W. A. de Heer, *Science* **297**, 787 (2002).

<sup>2</sup>Y. Cheng and O. Zhou, *C. R. Phys.* **4**, 1021 (2003).

<sup>3</sup>N. de Jonge and J.-M. Bonard, *Philos. Trans. R. Soc. London, Ser. A* **362**, 2239 (2004).

<sup>4</sup>N. I. Sinitsyn *et al.*, *Appl. Surf. Sci.* **111**, 145 (1997).

<sup>5</sup>A. N. Obraztsov, A. P. Volkov, and I. Pavlovsky, *Diamond Relat.*

*Mater.* **9**, 1190 (2000).

<sup>6</sup>K. A. Dean, P. vonAllmen, and B. R. Chalamala, *J. Vac. Sci. Technol. B* **17**, 1959 (1999).

<sup>7</sup>H. Ago, T. Kugler, F. Cacially, K. Petritsch, R. H. Friend, W. R. Salaneck, Y. Ono, T. Yamabe, and K. Tanaka, *Synth. Met.* **103**, 2494 (1999).

<sup>8</sup>S. Suzuki, C. Bower, Y. Watanabe, and O. Zhou, *Appl. Phys. Lett.* **76**, 4007 (2000).

<sup>9</sup>M. Shiraishi and M. Ata, *Carbon* **39**, 1913 (2001).

- <sup>10</sup>S. Suzuki, Y. Watanabe, Y. Homma, S. ya Fukuba, S. Heun, and A. Locatelli, *Appl. Phys. Lett.* **85**, 127 (2004).
- <sup>11</sup>O. Gröning, O. M. Küttel, C. Emmenegger, P. Gröning, and L. Schlapbach, *J. Vac. Sci. Technol. B* **18**, 665 (2000).
- <sup>12</sup>X. Cui, M. Freitag, R. Martel, L. Brus, and P. Avouris, *Nano Lett.* **3**, 783 (2003).
- <sup>13</sup>R. Gao, Z. Pan, and Z. L. Wang, *Appl. Phys. Lett.* **78**, 1757 (2001).
- <sup>14</sup>P. Gröning, L. Nilsson, P. Ruffieux, R. Clergereaux, and O. Gröning, in *Encyclopedia of Nanoscience and Nanotechnology*, edited by H. S. Nalwa (American Scientific Publishers, Stevenson Ranch, GA, 2004), Vol. 1, pp. 547–579.
- <sup>15</sup>M. J. Fransen, T. L. van Rooy, and P. Kruit, *Appl. Surf. Sci.* **146**, 312 (1999).
- <sup>16</sup>J. Zhao, J. Han, and J. P. Lu, *Phys. Rev. B* **65**, 193401 (2002).
- <sup>17</sup>B. Shan and K. Cho, *Phys. Rev. Lett.* **94**, 236602 (2005).
- <sup>18</sup>C. Herring and M. H. Nichols, *Rev. Mod. Phys.* **21**, 185 (1949).
- <sup>19</sup>K. L. Jiang, Q. Q. Li, and S. S. Fan, *Nature (London)* **419**, 801 (2002).
- <sup>20</sup>M. Zhang, K. R. Atkinson, and R. H. Baughman, *Science* **306**, 1358 (2004).
- <sup>21</sup>M. Zhang, S. Fang, A. A. Zakhidov, S. B. Lee, A. E. Aliev, C. D. Williams, K. R. Atkinson, and R. H. Baughman, *Science* **309**, 1215 (2005).
- <sup>22</sup>X. B. Zhang, K. L. Jiang, C. Feng, P. Liu, L. N. Zhang, J. Kong, T. H. Zhang, Q. Q. Li, and S. S. Fan, *Adv. Mater.*, doi: 10.1002/adma.200502528.
- <sup>23</sup>P. Li, K. L. Jiang, M. Liu, Q. Q. Li, and S. S. Fan, *Appl. Phys. Lett.* **82**, 1763 (2003).
- <sup>24</sup>A. L. Reimann, *Thermionic Emission* (Wiley, New York, 1934).
- <sup>25</sup>W. W. Dolan and W. P. Dyke, *Phys. Rev.* **95**, 327 (1954).
- <sup>26</sup>O. W. Richardson, *The Emission of Electricity from Hot Bodies*, 2nd ed. (Longmans, Green, and Co., London, 1921), Chap. 2, pp. 29–59.
- <sup>27</sup>L. W. Swanson and A. E. Bell, *Recent Advances in Field Electron Microscopy of Metals* (Academic Press, New York, 1973), Vol. 32, pp. 193–309.
- <sup>28</sup>M. Grujicic, G. Gao, and B. Gerstein, *Appl. Surf. Sci.* **206**, 167 (2003).
- <sup>29</sup>A. Maiti, J. Andzelm, N. Tanpipat, and P. vonAllmen, *Phys. Rev. Lett.* **87**, 155502 (2001).
- <sup>30</sup>G. Zhou, W. H. Duan, and B. L. Gu, *Phys. Rev. Lett.* **87**, 095504 (2001).
- <sup>31</sup>L. V. Whitney, *Phys. Rev.* **50**, 1154 (1936).